Unfolding of *Plasmodium falciparum* Triosephosphate Isomerase in Urea and Guanidinium Chloride: Evidence for a Novel Disulfide Exchange Reaction in a Covalently Cross-Linked Mutant†

Rajesh S. Gokhale,‡ Soumya S. Ray,‡ Hemalatha Balaram,§ and P. Balaram*,‡

Molecular Biophysics Unit, Indian Institute of Science, Bangalore 560012, India, and Molecular Biology and Genetics Unit, Jawaharlal Nehru Centre for Advanced Scientific Research, Jakkur Campus, Jakkur Post Office, Bangalore 560064, India

Received May 11, 1998; Revised Manuscript Received September 15, 1998

ABSTRACT: The conformational stability of *Plasmodium falciparum* triosephosphate isomerase (TIMWT) enzyme has been investigated in urea and guanidinium chloride (GdmCl) solutions using circular dichroism, fluorescence, and size-exclusion chromatography. The dimeric enzyme is remarkably stable in urea solutions. It retains considerable secondary, tertiary, and quaternary structure even in 8 M urea. In contrast, the unfolding transition is complete by 2.4 M GdmCl. Although the secondary as well as the tertiary interactions melt before the perturbation of the quaternary structure, these studies imply that the dissociation of the dimer into monomers ultimately leads to the collapse of the structure, suggesting that the interfacial interactions play a major role in determining multimeric protein stability. The C_m(urea)/C_m(GdmCl) ratio (where C_m is the concentration of the denaturant required at the transition midpoint) is unusually high for triosephosphate isomerase as compared to other monomeric and dimeric proteins. A disulfide cross-linked mutant protein (Y74C) engineered to form two disulfide cross-links across the interface (13-74′) and (13′-74) is dramatically destablized in urea. The unfolding transition is complete by 6 M urea and involves a novel mechanism of dimer dissociation through intramolecular thiol−disulfide exchange.

The folding of protein monomers and their assembly into functional oligomers is a fundamental step in the biosynthesis of multimeric proteins. Important questions that need to be addressed are the following: (1) Do completely active monomers associate to yield multimers or does association precede complete folding? (2) Can partially folded oligomeric states be populated as intermediates in the folding pathways? We have been examining the mechanistic features of the folding and unfolding of dimeric enzymes using disulfide interface mutants that abolish dissociation (*1*). Previous studies from this laboratory have shown that the covalent bridging of a fragile interface region in thymidylate synthase results in dramatic stabilization with respect to thermal and chaotrope-induced unfolding (*2*, *3*). Analysis of the three-dimensional structures of a large number of multimeric proteins suggests that the nature of interactions at protein interfaces may be similar to interactions observed between structural domains in multidomain proteins (*4*, *5*). Protein interfaces appear to contain substantially more polar interactions than the interior of well-packed globular proteins (*6*). It is therefore of particular interest to examine the effects of denaturants on intra- and intersubunit interactions. The availability of covalently cross-linked mutants permits a separation of the effects of dissociation and chain unfolding. We present in this report a detailed analysis of the unfolding behavior of the dimeric enzyme *Plasmodium falciparum* triosephosphate isomerase (TIMWT) in urea and guanidinium chloride (GdmCl), as well as the behaviour of a covalently cross-linked mutant containing two symmetry-related disulfide bridges across the subunit interface.

TIM is an attractive model system, since a large amount of structural and mechanistic information is available from studies of homologous TIMs from a variety of sources such as *Trypanosoma*, yeast, and chicken (*7*−*9*). In particular, studies aimed at engineering monomeric TIM have provided valuable information on the importance of specific interfacial interactions (*10*−*12*). TIM is a prototype of an eight-stranded α/*β*-barrel topology, in which the protein interface is primarily constituted of loops. These barrel enzymes have varying quaternary states and catalyze different types of reactions using substrates of distinct size and character. Interestingly, folding studies have been carried out extensively with monomeric barrel structures. In contrast, there are no detailed unfolding reports on mutimeric α/*β*-barrel proteins. The α-subunit of tryptophan synthase has been reported to have long-lived folding intermediates (*13*, *14*). On the basis of computer simulation studies, Skolnick and co-workers have suggested that such long-lived intermediates might be a characteristic of α/*β*-barrel proteins (*15*). However, the folding of monomeric fructose bisphosphate aldolase has more recently been shown to be a two-state process (*16*). Extensive work on *N*-(5′-phosphoribosyl)anthranilate isomerase has suggested that this class of proteins has a

† This work was supported by the Council of Scientific and Industrial Research, India (P.B.). R.S.G. was supported by a Senior Research Fellowship from the Council of Scientific and Industrial Research.

* Address correpondence to this author: FAX 91-80-3341683/91-80-3348535; E-mail pb@mbu.iisc.ernet.in.

‡ Indian Institute of Science.

§ Jawaharlal Nehru Centre for Advanced Scientific Research.

10.1021/bi981087s CCC: $18.00
Published on Web 12/12/1998

robust architecture, resilient to substantial sequence alterations (*17*). In contrast, most of the work on TIM, the epitome of the α/β-barrel family, have been focused primarily on understanding the mechanistic aspects of the isomerization reaction (*18*, *19*). Heteromeric TIMs have been generated from different sources by dissociation/reassociation experiments (*20*). Recently the refolding mechanism of rabbit muscle triosephosphate isomerase has been investigated in reverse micelles by fluorescence resonance energy transfer experiments (*21*). The studies demonstrated the appearance of an intermediate with high fluorescence quantum yield, which was suggested to be a partially folded monomer. Ligand binding to triosephosphate isomerase is found to enhance the stability against degradation by proteases (*22*). A preliminary folding study suggested that the folding pathway of the TIM dimer can be described by a consecutive first-order folding and second-order association reaction scheme, assuming inactive monomers (*23*). In a more recent report, unfolding studies of human TIM were carried out and the stability of the wild-type enzyme was compared with three interface mutants (*24*). The denaturation of wild-type human TIM was shown to be two-state in nature. Accumulation of equilibrium intermediates was not observed. The mutants were found to be less stable when compared with the wild-type enzyme. Further investigation with the human TIM mutants revealed that partial stability can be regained by mutations in the α-helical segments close to the dimer interface (*25*). However, there are no detailed kinetic or equilibrium unfolding studies available for triosephosphate isomerases from other species.

Triosephosphate isomerase (TIMWT) from the malarial parasite *Plasmodium falciparum* is a homodimer with a monomer molecular mass ~27 kDa. The TIM gene from *P. falciparum* has been cloned and expressed in *Escherichia coli* (*26*). The crystal structure of this protein has been determined at 2.2 Å resolution (*27*). Understanding the folding and assembly of the parasite enzyme may be of importance in designing molecules that can impede association of the subunits. Since enzyme active sites are highly conserved between host and parasite, interface disruption strategies may provide a viable route toward potentially useful inhibitors of multimeric enzymes (*28*). The equilibrium unfolding studies of *Plasmodium falciparum* triosephosphate isomerase (TIMWT) described in this report establish the absence of complete dissociation and the presence of considerable secondary and limited tertiary structure, even in 8 M urea. In contrast, TIMWT is completely unfolded in 2.4 M GdmCl solution. Interestingly, an intermediate characterized as an aggregate appears at low concentrations (0.8−1.2 M) of GdmCl. A bisdisulfide mutant (Y74C) protein (Y74Cox), constructed based on modeling such that two disulfide bridges (13-74′ and 74-13′) are formed by using the preexisting Cys13 residue at the dimer interface, was found to be surprisingly unstable in urea solutions. Gel filtration and SDS−PAGE of urea-treated protein samples established a novel way of dissociation by intramolecular thiol−disulfide exchange, resulting in the reduction of intersubunit disulfide bridges. The maintenance of quaternary structure of the protein appears critical for the stability of the enzyme.

MATERIALS AND METHODS

Purification of TIMWT. The *Plasmodium falciparum* triosephosphate isomerase gene was cloned into a pTrc 99A vector, called pARC1008 (*26*). The protein is overexpressed in the *E. coli* strain AA200, which has a null mutation in the host TIM gene (*29*). This was provided to us by the Astra Research Centre, India. The purification of TIM involves a two-step protocol. In the first step the cell lysate is subjected to ammonium sulfate precipitation, where TIMWT could be selectively precipitated at 95% saturated ammonium sulfate (63% w/v). Following this, the protein was further purified by ion-exchange chromatography on a Pharmacia FPLC system. The detailed purification procedure has been described before (*27*). Yields up to 125 mg/L of *E. coli* culture were routinely obtained.

The site-directed mutant Y74C was constructed by the method of Kunkel (*30*). The mutant was purified in a similar way. Purified protein yields between 80 and 90 mg/L of *E. coli* culture were obtained for the mutant. The oxidation of the mutant to Y74Cox was carried out by air oxidation using extensive dialysis in 20 mM Tris-HCl (pH 8.0) for 24 h. A protein concentration of less than 1 mg/mL was used for dialysis. The purified enzyme was found to have a specific activity of 7800−8000 units/mg of protein.

Reagents. Urea was recrystallized from hot boiling ethanol. After filtration, urea crystals were dried in a vacuum oven at 30 °C. Urea stocks were prepared fresh before each experiment. GdmCl (Sigma) was used directly for unfolding studies. All other chemicals were of analytical grade.

Circular Dichroism. Protein (8 μM) was incubated for at least 1 h at the required urea/GdmCl concentration in 100 mM Tris-HCl buffer, pH 8.0, before the spectrum was recorded. Preliminary studies confirmed that equilibrium was reached within $^1/_2$ h of incubation. Circluar dichroism measurements were carried out on a Jasco J500A spectropolarimeter. Ellipticity changes at 220 nm were monitored to follow the far-UV unfolding transition, with a path length of 1 mm. The near-UV band was followed with a 5 mm path length cuvette, at a protein concentration of 28 μM. Spectra were averaged over 2−4 scans at a scan speed of 10 nm/min. Unfolding transitions were followed by monitoring ellipticity at 280 nm.

Fluorescence Spectroscopy. Emission spectra were recorded on a Hitachi 650-60 spectrofluorimeter. Intrinsic tryptophan fluorescence was monitored at varying concentrations of urea in 100 mM Tris-HCl (pH 8.0). Equilibration was achieved within $^1/_2$ h of incubation. Protein samples were excited at 280 nm and the emission was monitored at 331 nm. Excitation and emission band-pass were set at 5 nm. Urea unfolding studies were carried out at a protein concentration of 4 μM, while GdmCl unfolding was carried out over a range of protein concentration from 2 to 8 μM.

Size-Exclusion Gel Chromatography. Gel-filtration experiments were carried out on a Superose 6B column with an exclusion limit of 4×10^6 Da for proteins using a Pharmacia FPLC system. The void volume of the column was 10 mL. The elution of the protein was detected at 280 nm. The protein (20 μM) was incubated for 1 h at the required urea/GdmCl concentration and in 100 mM Tris-HCl (pH 8.0). A 50 μL aliquot of this sample was injected on the column with 100 mM Tris-HCl (pH 8.0) at the

required denaturant concentration. A uniform concentration of 150 mM NaCl was used for column equilibration at all denaturant concentrations to prevent nonspecific binding of protein to the column material. The flow rate was adjusted to 0.4 mL/min.

SDS−PAGE Analysis of TIM Unfolding. The oxidized form of the mutant Y74C was incubated with increasing urea concentrations in 100 mM Tris-HCl (pH 8.0) for 1 h at room temperature. Following this, the protein was loaded on a nonreducing SDS−polyacrylamide (12%) gel and electrophoresed. Staining with Coomassie blue R was carried out to visualize the protein bands.

Carboxamidomethylation of Y74Cox. Y74Cox (20 mg/mL) was incubated with 0.6 M iodoacetamide in 100 mM Tris-HCl, pH 8.0, for 2 h with intermittent agitation. Following this, the excess iodoacetamide was separated from the labeled protein on a 10 mL Sephadex G10 desalting column. The protein elutes in the void volume of the column. The labeled protein on thiol estimation showed <1 thiol group/dimer. TIMWT yielded a thiol value of 4/monomer, which is in agreement with the sequence. Thiol estimation was carried out with Ellman's reagent (*31*).

RESULTS

Expression, Purification, and Enzymatic Activity. Recombinant *Plasmodium falciparum* TIM cDNA was overexpressed in *E. coli* and the protein was purified by collecting the 70−95% ammonium sulfate fraction, followed by FPLC on a Mono Q column. A batch of 1 L of culture yielded 125 mg of purified protein. The two-step protocol yielded highly purified protein from crude cell extracts. The protein is seen as a ∼27 kDa band on SDS−PAGE (data not shown) and the matrix-assisted laser desorption ionization time-of-flight (MALDI-TOF) spectrum yielded a molecular weight of 27 840 Da. Analysis of TIMWT by electrospray mass spectrometry (data not shown) further demonstrated that the protein has a mass of 27 832 Da. The calculated molecular mass of TIMWT from the published sequence (*26*) is found to be 27 935 Da. The disagreement between the observed and the calculated masses may be accounted for by assuming that Met1 is lost from the protein expressed in *E. coli*. Further, the crystal structure shows absence of electron density for the first three residues and presence of valine at position 163 (alanine in DNA sequence) (*27*). It was reasoned that incorporation of valine in place of alanine was due to a translational error during overexpression of TIMWT. Such translation errors have been reported in several cases during overexpression of heterologous proteins in *E. coli* (*32*, *33*). The calculated mass of TIMWT having Met1 deleted and bearing A163V mutation is 27 832 Da, in agreement with the mass spectral data. The purified enzyme was found to have a specific activity of 7800−8000 units/mg of protein.

Unfolding of TIMWT: (A) Unfolding in Urea. (i) Intrinsic Tryptophan Fluorescence. TIMWT has two tryptophans in each monomer, at positions 11 and 168. The crystal structure of PfTIM reveals that Trp 11 is present at the interface, whereas Trp 168 is present in the mobile active-site loop 6. In addition, there are seven Tyr residues per monomer in TIMWT. Excitation at 280 nm results in an emission maximum at 331 nm. The emission maximum is unaffected by a shift in excitation wavelength to 295 nm, suggesting the overwhelming contribution of the Trp residues to the emission spectrum. The emission maximum of TIMWT at pH 8.0 at 331 nm suggests that both these fluorophores are in relatively hydrophobic environments. This is consistent with the surface accessibility values for the two tryptophans determined from the crystal structure (*27*). In 8 M urea solutions the emission maximum shifts to 340 nm. Normally, buried Trp residues in folded proteins show a fluorescence emission maximum of 330−340 nm, while exposed Trp residues yield emission maxima between 348 and 356 nm (*34*). The observed 340 nm emission maximum in 8 M urea for TIMWT suggests that, even at these denaturant concentrations, one or both Trp residues are still in a largely hydrophobic environment in TIMWT. The spectrum of TIMWT recorded in 6 M GdmCl (discussed later) shows an emission maximum of 356 nm, indicative of the complete exposure of the Trp residues.

Figure 1a shows the changes in the intrinsic tryptophan fluorescence of TIMWT monitored as a function of urea concentration along with the fraction unfolded, calculated from the raw data. Very small wavelength changes are observed in the region of 0−6 M urea with the emission maximum shifting from 331 to 333 nm. Above 6 M urea, there is a sharp shift in the spectral maximum, with a limiting value of 340 nm being obtained at 8 M urea. Figure 1b shows that up to 6 M urea almost 40% of the original emission intensity is still retained. However, there is a sharp fall in the emission yields between 6 and 8 M urea. The gradual changes in the spectroscopic properties over the range of 0−6 M urea are suggestive of incremental changes of the structure and absence of a sharp transition between well-characterized folded and unfolded states. Between 6 and 8 M urea the environments of the Trp residues appear to undergo a significant change.

(ii) Circular Dichroism. The native protein has a prominent negative band at 220 nm. With increasing urea concentration there is a reduction in the ellipticity of the CD bands without any significant change in the shape of the spectrum. Interestingly, even at 8 M urea there is significant far-UV CD ellipticity, suggesting that appreciable secondary structure is still maintained. Figure 2a shows the ellipticity at 220 nm plotted as a function of urea concentration. It is clearly seen that there is no sharp unfolding transition detected by far-UV CD, suggestive of a complex multistep process. The near-UV CD spectra of TIMWT shows a negative CD band centered at 280 nm, which may be assigned to the two Trp residues and seven Tyr residues in the protein. Figure 2b shows near-UV CD ellipticities plotted as a function of urea concentration. A sharp transition is observed between 4.8 and 8.0 M urea. Even in 8 M urea some residual near-UV CD ellipticity is still observed, suggesting that complete loss of tertiary structure is not achieved under these conditions.

Taken together, the far-UV and near-UV CD results demonstrate the presence of significant secondary and tertiary interactions in TIMWT even in 8 M urea solution. This suggests that the TIM α/β barrel is a particularly robust structure that does not unfold completely even at high urea concentrations. It is interesting to note that there is noncoincidence of the far-UV and near-UV unfolding curves, suggesting the presence of folding intermediates. The presence of significant secondary and tertiary interactions

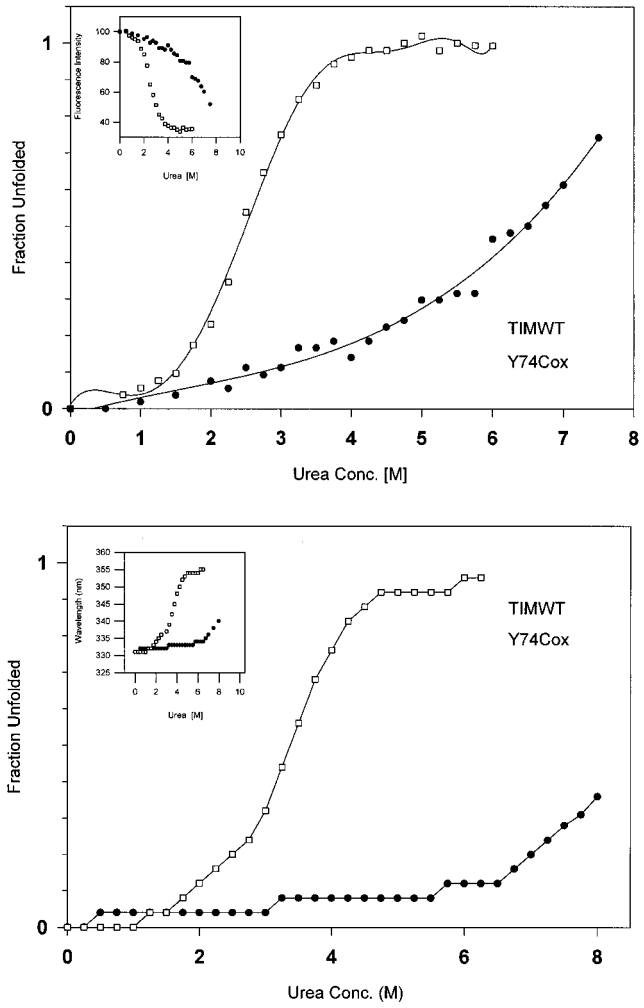

FIGURE 1: (a, top) Urea unfolding of TIMWT (●) and Y74C (□) monitored by following intrinsic tryptophan fluorescence at 25 °C, pH 8.0. Protein concentrations were 4 mM in 100 mM Tris-HCl, pH 8.0. The main panel shows the fraction unfolded for TIMWT and Y74C plotted as a function of urea concentration. Since the unfolding transition of TIMWT in urea is incomplete, the fraction unfolded was calculated by using the unfolding baseline of Y74Cox. The mutant protein is completely unfolded by 6 M urea. The inset shows the raw data used for calculation of fraction unfolded. Dependence of fluorescence intensity (331 nm) at varying urea concentrations is plotted in the inset. The plot is normalized by taking the fluorescence intensity at 0 M urea as 100%. (b, bottom) Urea unfolding of TIMWT (●) and Y74C (□) monitored by following intrinsic tryptophan fluorescence at 25 °C, pH 8.0. Protein concentrations were 4 mM in 100 mM Tris-HCl, pH 8.0. The main panel shows the fraction unfolded for TIMWT and Y74C plotted as a function of urea concentration. Since the unfolding transition of TIMWT in urea is incomplete, the fraction unfolded was calculated by using the unfolding baseline of Y74Cox (356 nm). The inset shows the dependence of fluorescence emission at varying urea concentrations. The emisson maximum of the folded protein is at 331 nm, which is used for subsequent calculations.

has been demonstrated in 6−8 M urea solutions in the case of FK-506 binding protein (*35*) and bacteriophage 434 repressor (*36*).

(iii) Size-Exclusion Chromatography. Partially unfolded states of proteins have been known to aggregate at intermediate denaturant concentrations (*37, 38*). To characterize the quaternary state of TIMWT in urea solutions, size-exclusion chromatography experiments were performed. Figure 3a summarizes the results of gel-filtration experiments carried out in urea solution on a Superose 6B FPLC column. The

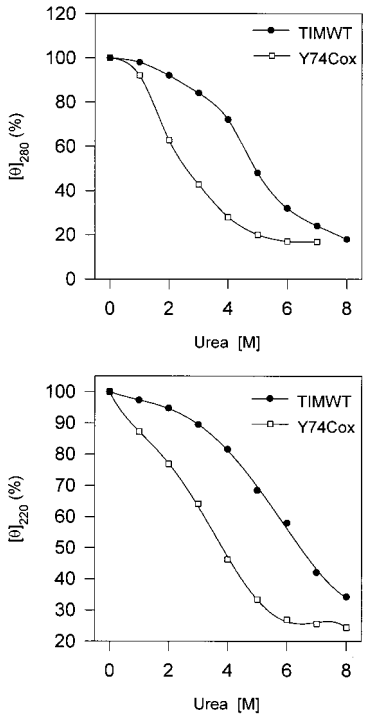

FIGURE 2: (a, top) Dependence of CD ellipticity of TIMWT and Y74Cox at 220 nm (θ_{220}) as a function of urea concentration at 25 °C, pH 8.0. Protein concentrations were 8 μM (100 mM Tris-HCl, pH 8.0) and the path length was 0.1 mm. The ellipticity value in absence of denaturant was taken as 100%. (b, bottom) Plot of unfolding transition of TIMWT as a function of urea concentration. Unfolding was monitored by near-UV CD at 280 nm at 25 °C, pH 8.0. Protein concentrations were 28 mM and the path length was 5 mm. The ellipticity at 0 M urea is taken as 100%.

native dimeric species (peak A) can be observed even in 8 M urea, albeit at a decreased elution volume of 16 mL, as compared to 16.2 mL in the absence of urea. A new peak B begins to elute in 5 M urea at 14.8 mL. Peak B becomes significant in 8 M urea and elutes at 14.5 mL. The area under the two peaks is approximately equal in 8 M urea. Peak B, which elutes ahead of the native dimeric species, probably corresponds to a highly solvated unfolded monomer. It is pertinent to note that a partially unfolded dimer cannot be excluded at this stage. The observation that the unfolded monomer of TIM elutes earlier than the solvated folded dimer is consistent with previous studies on the multimeric enzyme *Lactobacillus casei* thymidylate synthase (*2*) and pyruvate decarboxylase (*39*). The presence of two peaks at a urea concentration ≥5 M indicates that equilibration between folded dimer and unfolded monomer species is slow compared to the time scale of chromatography.

(B) Unfolding in GdmCl. (i) Intrinsic Tryptophan Fluorescence. Equilibrium unfolding studies of TIMWT were performed in GdmCl solutions to compare its conformational stability in a relatively stronger denaturant. Figure 4a shows the unfolding profile obtained by using intrinsic fluorescence. TIMWT is completely unfolded by 2 M GdmCl. It is noteworthy that there is a slight increase in the fluorescence intensity between 0.8 and 1.2 M GdmCl, suggesting the presence of an intermediate. The increase in the fluorescence intensity may be due to burial of the tryptophan residues in a hydrophobic environment. However there is no blue shift in the spectrum observed. Figure 4b summarizes unfolding studies carried out at various protein concentrations. The

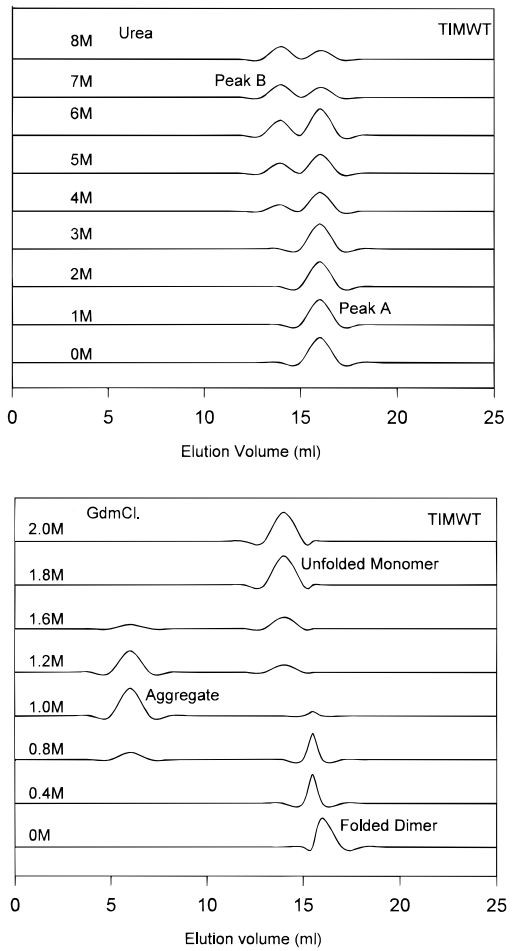

FIGURE 3: (a, top) Size-exclusion gel chromatography profile of TIMWT carried out on a Superose 6B column following equilibration of the column at the desired urea concentration (100 mM Tris-HCl, pH 8.0). Samples were incubated at the desired urea concentration before injection onto the column. The elution of the protein was monitored by measuring absorbance at 280 nm. (b, bottom) Size-exclusion gel chromatography profile of TIMWT carried out on a Superose 6B column following equlibration of the column at the desired GdmCl concentration (100 mM Tris-HCl, pH 8.0). Samples were incubated at the desired GdmCl concentration before injection onto the column. The elution of the protein was monitored by measuring absorbance at 280 nm. The void volume of the column was measured with blue dextran (mol wt 200 000 Da).

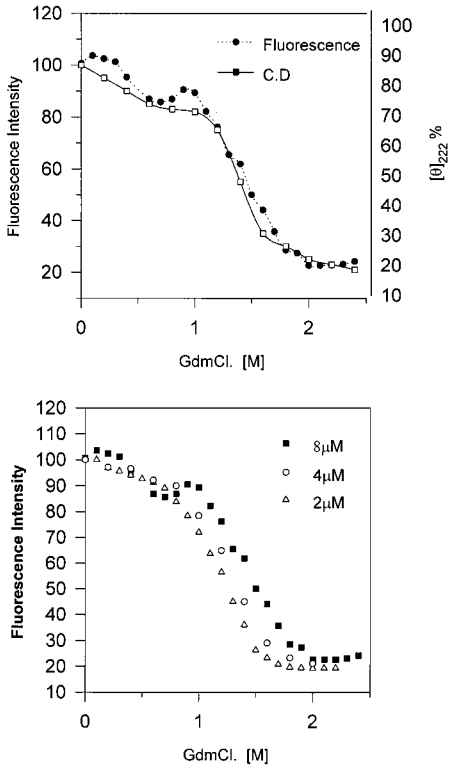

FIGURE 4: (a, top) Unfolding of TIMWT in GdmCl solution was monitored by intrinsic tryptophan fluorescence intensity and far-UV CD. The other experimental conditions were identical to those in the urea unfolding experiments in Figures 2 and 3. Both the CD and the fluorescence unfolding curves were normalized by taking the spectroscopic parameter to be 100% in absence of any denaturant. The *y*-axis on the left of the panel indicates the fluorescence intensity (331 nm), while changes in molar ellipticity, θ_{220}, are indicated on the right. (b, bottom) Unfolding of TIMWT in GdmCl was monitored as a function of protein concentration using intrinsic tryptophan fluorescence. The protein concentrations used were 2, 4, and 8 μM. The protein samples were incubated in 100 mM Tris-HCl, pH 8.0, at the appropiate GdmCl concentration for 1 h prior to measurement of fluorescence.

results show a strong protein concentration dependence of this intermediate population, suggesting aggregation at low GdmCl concentration. Appearance of aggregates at low GdmCl concentrations has been observed in the case of other multimeric proteins such as glyceraldehyde-3-phosphate dehydrogenase (*40*) and pyruvate dehydrogenase (*41*).

(ii) Circular Dichroism. Far-UV CD studies also show a pronounced loss of secondary structure by 2 M GdmCl (Figure 4a). Interestingly, near-UV CD studies, which require high protein concentration (28 μM), resulted in protein precipitation for GdmCl concentrations ranging from 0.1 to 0.6 M. This result suggests that the initial perturbation of the structure by GdmCl probably result in exposure of certain segments leading to the formation of aggregation-competent intermediates, resulting in precipitation at higher concentrations. Such effects have been observed earlier in the case of creatinase (*42*, *43*).

(iii) Size-Exclusion Chromatography. Gel filtration carried out on a Superose 6B FPLC is summarized in Figure 3b. At a relatively low concentration of GdmCl (0.8−1.4 M), a peak is observed in the void volume of the column that presumably corresponds to a high molecular weight aggregate (exclusion limit 4×10^6 Da). Folded TIMWT elutes at 16.2 mL. At higher GdmCl concentrations (>1.6 M) both TIMWT and the aggregates are no longer observed and a new peak at 14.5 mL is seen. This may be assumed to be a completely unfolded monomeric species.

Modeling of the Disulfide Mutant. To define the order in which subunit dissociation and chain unfolding occurs in denaturant solution, a mutant bearing covalent cross-links between the two subunits was designed. The introduction of appropriately positioned cysteine residues at the dimer interface should, in principle, permit covalent cross-linking upon disulfide bond formation. PfTIM (TIMWT) contains a cysteine residue at position 13 that forms part of the dimer interface. By use of the disulfide modeling program MODIP (*44*) developed earlier in our laboratory, Tyr74′ on the neighboring subunit was identified as a suitable candidate for mutation to Cys. Since modeling was carried out prior to the structure determination of PfTIM, coordinates of trypanosomal TIM (5TIM) were used. This was justified

since there is a high homology (40%) between the sequences, suggesting that the proteins may have similar tertiary structure. Disulfide modeling using the susequently determined PfTIM coordinates (*27*) have indeed validated the choice of Tyr74 as a candidate for mutation.

Purification and Characterization of Y74C. The mutant protein Y74C was purified by the same purification protocol followed for TIMWT and was obtained in high yield. The mutant protein was air-oxidized to a covalently bridged dimer (Y74Cox) that had the expected values for free thiols (3/monomer) and was observed as a 56 kDa protein on nonreducing SDS−PAGE (data not shown). The specific activity of the protein was found to be 8426 units/mg (94% of the TIMWT). The UV, fluorescence, and CD spectra were almost identical to those of TIMWT, suggesting that the mutation had not resulted in any significant alteration of protein structure.

Unfolding of Y74C in Urea: (i) Intrinsic Tryptophan Fluorescence. Figure 1a shows the changes in Trp fluorescence intensity at varying urea concentrations. The mutant protein Y74Cox shows a sharp two-state unfolding profile, in contrast to wild-type protein, which has a broad transition. The unfolding transition midpoints are centered at 3.5 and 5.5 M urea for Y74Cox and TIMWT, respectively. The changes in the emission wavelength maximum are shown in the inset of Figure 1b. TIMWT has an emission maximum of 340 nm even in 8 M urea. Y74Cox, on the other hand, has an emission wavelength of 354 nm in 5 M urea, indicative of the complete exposure of the tryptophan residues.

Urea unfolding profiles of Y74Cox in urea solution obtained by fluorescence and CD approximate a two-state transition and do not show the presence of stable intermediates over a wide range of denaturant concentrations. This is contrast to the wild-type protein, where the unfolding results in gradual change in spectroscopic properties.

(ii) Circular Dichroism. Figure 2a shows the unfolding profiles of Y74Cox and TIMWT followed by monitoring the changes in the far UV CD spectrum (molar ellipticity at 220 nm). The transition curves show that Y74Cox tends to unfold at a very low urea concentration with a distinct two-state transition. The midpoint of transition is centered around 3.5 M urea, in contrast to TIMWT, which has a transition midpoint at around 5.8 M (TIMWT does not completely unfold by 8 M urea; thus it is difficult to find the exact midpoint of transition). Instead of the broad unfolding profile of TIMWT, the mutant protein shows a sharp transition betwen 3 and 5 M urea. Most of the secondary structure in Y74Cox is lost by 6 M urea. Figure 2b compares the near UV CD unfolding profiles of Y74Cox with TIMWT at 280 nm. Here again, the ellipticity falls much more sharply for the mutant protein. The midpoint of transition of Y74Cox and TIMWT are observed at 2.4 and 4 M urea.

(iii) SDS−PAGE Analysis of Urea Denaturation. Figure 5a shows the electrophoretic pattern for Y74Cox at various urea concentrations under *nonreducing* conditions. In the absence of urea, Y74Cox migrates at an apparent molecular mass of 56 kDa, clearly corresponding to the covalently cross-linked dimer. Surprisingly, at urea concentrations >3 M, the dimer band diminishes in intensity, while a new band corresponding to the monomer appears. *This is possible only when the disulfide bridges across the interface are reduced*.

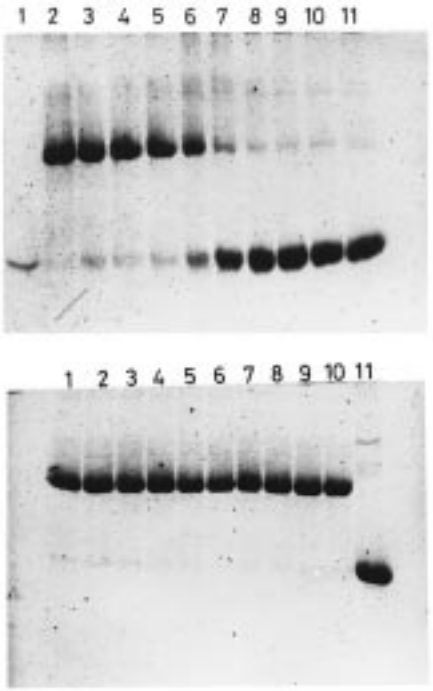

FIGURE 5: (a, top) Nonreducing SDS−PAGE of TIMMox following incubation at increasing urea concentrations at 50 mM Tris-HCl, pH 8.0. Lane 1 is TIMWT (marker for monomeric TIM) and lane 2 is TIMMox (marker for dimeric TIM). Lanes 3−10 correspond to TIMMox incubated at various urea concentrations: lane 3, 0 M; lane 4, 1 M; lane 5, 2 M; lane 6, 3 M; lane 7, 4 M; lane 8, 5 M; lane 9, 6 M; lane 10, 7 M; and lane 11, 8 M. (b, bottom) Nonreducing SDS−PAGE of carboxamidomethylated TIMMox following incubation at increasing urea concentrations. All experimental conditions were the same as in panel a except that the protein TIMMox was alkylated with iodoacetamide prior to incubation in urea solution. Here, lanes 1−9 correspond to the protein incubated at various urea concentrations ranging from 0 to 8 M. Lanes 10 and 11 are controls for monitoring the mobility of dimeric (TIMMox, 0 M) and monomeric (TIMWT) protein.

Inspection of the amino acid sequence of TIMWT shows that there are four cysteine residues present in each monomer. Formation of two disulfide bridges between preexisting Cys13 and the newly introduced Cys74 results in six free thiols in the dimeric protein. The observation of monomeric bands at >3.0 M urea is probably the result of thiol−disulfide exchange. The possibility of thiol−disulfide exchange occurring by nucleophilic attack of thiols from the other subunit is ruled out, as this would have again resulted in cross-linked dimeric protein. To obtain monomers, exchange should result by attack of a free Cys on the disulfide-bonded Cys *from the same subunit*. The occurrence of thiol−disulfide exchange was further supported by carboxamidomethylation of the free cysteines by iodoacetamide. This carboxamidomethylated Y74Cox showed only a single dimeric band at urea concentrations up to 8 M (Figure 5b). Lowering the pH to 6.0 reduced the observed monomerization at urea concentrations >3 M significantly, suggesting that alteration of nucleophilicity of the free thiol resulted in diminished exchange.

(iv) Size-Exclusion Chromatography. To further examine the nature of the intermediates during the thiol−disulfide exchange, gel filtration studies were carried out. Figure 6 shows the chromatographic profiles of Y74Cox at varying urea concentrations. The mutant protein shows as many as

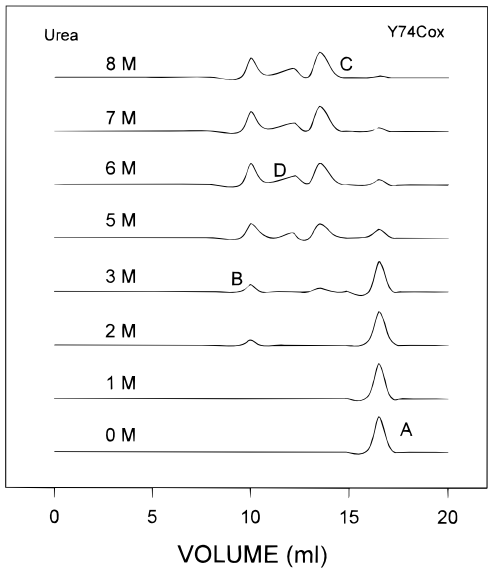

FIGURE 6: Size-exclusion gel chromatography of TIMMox carried out on a Superose 6B gel-filtration column. The column was preequilibrated with the desired urea concentration (100 mM Tris-HCl, pH 8.0). The protein sample was incubated at the same urea concentration as that of the column for 1 h before injection.

four peaks at >4 M urea, viz., 16 mL (peak A), corresponding to the folded dimer; 14.1 mL (peak C), which is probably similar to unfolded monomer; and 7.0 mL (peak B) in the void volume of the column, corresponding to an aggregated species. Peak D eluting between peaks B and C may correspond to partially unfolded monomer following disulfide exchange. Clearly the unfolding of Y74Cox in urea is characterized by several unusual features. In *P. falciparum* TIM there are four thiols per monomer (Cys13, Cys126, Cys196, and Cys217). The analysis of the crystal structure shows that Cys126 is closest to the engineered disulfide. The multiple peaks observed during the unfolding of Y74C in urea may be due to unfolding intermediates resulting from thiol−disulfide exchange reactions with more than one Cys residue. The occurrence of several intermediates with various elution volumes has been observed during the unfolding of several disulfide-containing proteins such as ribonuclease T1 (*45*), bovine pancreatic trypsin inhibitor (BPTI) (*46*), and α-lactalbumin (*47*).

DISCUSSION

The conformational stability of multimeric proteins can be measured by equilibrium unfolding studies in urea and GdmCl solutions. The unfolding of TIMWT in urea and GdmCl suggests dramatically different unfolding pathways and mechanisms in the two denaturants. The two possible unfolding pathways in urea and guanidium are represented schematically in Figure 7. In urea the protein is quite robust and does not unfold even at a denaturant concentration of 8 M. In sharp contrast the protein is completely unfolded by 2 M GdmCl. In principle, tertiary and quaternary structures are stabilized by virtually similar interactions. Therefore, the dissociation of oligomeric protein by denaturants will cause at least partial unfolding of subunits. Even at very low GdmCl (up to 0.6 M), there is partial unfolding with a decrease in far UV CD and a minor increase in fluorescence intensity. These changes result from the exposure of aggregation-competent segments as seen from concentration

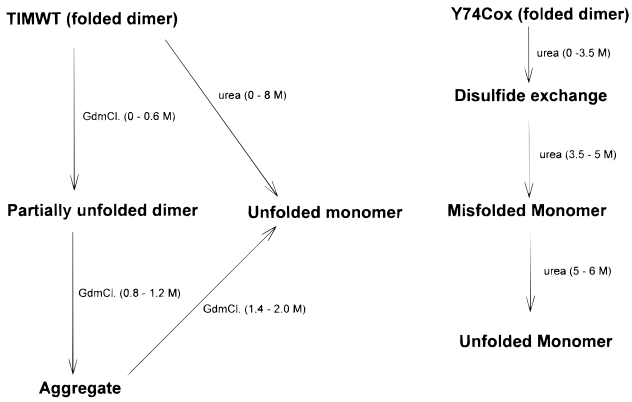

FIGURE 7: Schematic unfolding pathway of TIMWT in urea and GdmCl and Y74C in urea.

dependence of unfolding and gel-filtration studies. This aggregation is abolished at higher GdmCl concentrations due to breakdown of the aggregate to unfolded monomer. The structure of the TIM barrel breaks down completely by 2.1 M GdmCl, with the midpoint of transition at 1.5−1.6 M GdmCl. Although the detailed mode of interaction of the two denaturants is not clear, GdmCl always unfolds polypeptide chains at a much lower concentration than urea. Generally, proteins denature in the range of 4−6 M urea and 2−3 M GdmCl. The midpoints of transition (C_m) of some well-studied proteins are compared in Table 1. For most monomeric proteins, unfolding in urea occurs at a concentration twice that required in case of GdmCl (with the exception of maltose binding protein), suggestive of a "2-fold rule". Multimeric proteins on the other hand have a higher ratio [C_m(urea)/C_m(GdmCl)] (with the exception of bovine growth hormone). This suggests that multimeric proteins may be more susceptible to GdmCl-induced unfolding. For proteins with non-two-state transitions the C_m value may not be an accurate measure of the stability to chaotrope; however, C_m values provide some indications for the differences in the interactions of the denaturants with different classes of proteins. The greater facility for GdmCl-induced denaturation in the case of oligomers is consistent with the view that the protein interfaces are appreciably more polar than the core of the protein (*6*). Interestingly, the test case (TIMWT) here shows dramatic differences in unfolding characteristics in the two denaturants. TIMWT can therefore be used as a model to clarify the effect of the two denaturants on the protein structure. GdmCl, being an ionic molecule, is expected to have a stronger destabilizing effect on polar interactions in protein structures, as compared to urea. Studies on small α-helices have demonstrated that GdmCl is twice as effective as a denaturant compared to urea on a molar basis. Equimolar concentrations of urea and salts are found just as effective as GdmCl in unfolding α-helices (*48*). Urea unfolding of TIMWT was carried out in the presence of several salts such as 1 M KCl and 1 M $(NH_4)_2SO_4$, but salts in combination with urea failed to reproduce the effects of GdmCl (data not shown). Calorimetric studies of ribonuclease, hen egg white lysozyme, and cytochrome *c* suggest that "binding sites for urea and GdmCl are likely to be formed by hydrogen bonding groups" (*49*).

The unfolding studies presented here suggest that the dimeric state of TIMWT is critical in maintaining the overall stability of the protein. In both these denaturants, the

Table 1: Comparison of Urea and Guanidinium Chloride C_m Values for Proteins[a]

protein	oligomeric state	C_m (urea, M)	C_m (GdmCl, M)	C_m (urea)/C_m (GdmCl)	ref
RNase A	monomer	6.6	3.0	2.2	*50*
RNase T1	monomer	4.6	2.9	1.59	*50*
Arc repressor	monomer	2.65	1.4	1.89	*51*
barnase	monomer	4.57	1.97	2.31	*52*
barstar	monomer	3.76	1.8	2.08	*53*
PMS-CT	monomer	4.3	2.0	2.31	*54*
maltose binding protein	monomer	3.5	1.05	3.33	*55, 56*
phosphoglycerate kinase	monomer	2.0	0.9	2.22	*57*
cytochrome P450	monomer	2.8	1.5	1.86	*58*
ferric enterobactin	monomer	5.98	1.95	3.06	*59*
myoglobin	monomer	5	1.5	3.33	*61*
tryptophan synthase	monomer	4.0	1.9	2.1	*60*
thioredoxin	monomer	5.6	2.5	2.24	*61*
bovine growth hormone	dimer	8.3	3.8	2.1	*62, 63*
invertase	dimer	5.25	1.6	3.28	*64*
glutathione transferase	dimer	5.5	1.5	3.66	*65*
dipeptidyl peptidase IV	dimer	>6	1.8	3.33	*66*
creatinase	dimer	5.2	2.0	2.6	*67*
vitronectin	tetramer	6.0	2.8	2.1	*68*
phosphofructokinase	tetramer	2.8	0.6	4.6	*69*
thymidylate synthase	dimer	5.8	1.8	3.22	*1*
triosephosphate isomerase	dimer	>6.0	1.4	>4.3	this work

[a] C_m is the denaturant concentration at the midpoint of transition.

initiation of the dissociation spurs the major transitions in the secondary and tertiary interactions. It is therefore likely that GdmCl destabilizes some of the critical polar interaction at the interface. The crystal structure of PfTIM (*27*) suggests that there are a number of critical intersubunit polar contacts within a 4 Å distance that might contribute largely to this susceptibility to GdmCl. Another interesting feature is the appearance of an aggregate at low GdmCl concentrations. The small but significant increase in C_m value determined for GdmCl unfolding upon increasing protein concentration may be interpreted as evidence for dissociation to precede chain unfolding. However, consideration of the results presented in Figure 4B suggest that, even at low concentrations of GdmCl (0.8 M), significant aggregation is observed in gel-filtration experiments. Protein association leading to off-pathway aggregation mediated by partially unfolded structures must also be considered. The small increment in the fluorescence intensity observed at 0.8 M GdmCl may in fact argue for the presence of off-pathway aggregation in this study. Previously, studies on thymidylate synthase suggested that fragile regions of the dimer interface may be involved in aggregation (*1*, *2*). Covalent bridging of the dimer interface by disulfide bonds abolished aggregation (*2*). Fluorescence studies on TIMWT suggested the presence of a tryptophan residues (Trp11 or Trp168) in the aggregation-competent structure.

A bisdisulfide cross-linked mutant Y74Cox was designed to provide a mutant in which subunit dissociation was not possible. Whereas the mutant was designed to prevent subunit dissociation, the covalently cross-linked Y74Cox was found to be *surprisingly labile as* compared to TIMWT. Spectroscopic data unambiguously demonstrate the unfolding of Y74Cox at 5.5−6.0 M urea. Gel filtration and SDS−PAGE of urea-unfolded protein establishes that the *monomerization* of Y74Cox occurs during urea unfolding (4.0 M). Even more surprisingly, the covalently cross-linked dimer interface mutant monomerizes *in the absence of any reducing agent* at intermediate urea concentrations, again supporting the fact that the quaternary state of the protein is critical for its overall stability. The only viable explanation for this observation appears to be that a free thiol group on the protein exchanges with the intersubunit disulfide resulting in an *intrasubunit nonnative disulfide.* Disulfide exchange reactions during unfolding reactions are well-known in several cases, especially in α-lactalbumin and BPTI (*42*, *43*). This interpretation is supported by the fact that monomerization as monitored by the nonreducing SDS−PAGE is abolished by prior carboxamidomethylation of the free thiols and by much lower yields of monomer at lower pH. This unusual thiol−disulfide exchange precludes a quantitative comparison of urea unfolding studies of the wild type and the mutant protein. These observations suggests that further characterization of the nonnative disulfide-containing TIM may throw light on the structural changes accompanying the urea-induced unfolding.

ACKNOWLEDGMENT

We are grateful to the Astra Research Center, India, for providing the clone of *Plasmodium falciparum* triosephosphate isomerase. We are grateful to Dr. M. K. Mathew, National Center for Biological Sciences (TIFR), Bangalore, India, for the use of the FPLC system. We also thank Dr. P. Humphrey (Kratos Analytical, UK) for providing the MALDI spectra of TIMWT and Dr. David King (University of California, Berkeley) for the ESI-MS spectra of TIMWT and for many helpful comments on the mass spectral data. P.B. is an honorary professor of the Jawaharlal Nehru Centre for Advanced Scientific Research.

REFERENCES

1. Gokhale, R. S., Agarwalla, S., Santi, D. V., and Balaram, P. (1996) *Biochemistry 35*, 7150−7158.
2. Agarwalla, S., Gokhale, R. S., Santi, D. V., and Balaram, P. (1996) *Protein Sci. 5*, 270−277.
3. Gokhale, R. S., Agarwalla, S., Francis, V. S., Santi, D. V., and Balaram, P. (1994) *J. Mol. Biol. 235*, 89−94.
4. Miller, S., Lesk, A. M., and Chothia, C. (1987) *Nature 328*, 834−836.

5. Argos, P. (1988) *Protein Eng. 2*, 101−113.
6. Jones, S., and Thornton, J. M. (1995) *Prog. Biophys. Mol. Biol. 63*, 31−65.
7. Banner, D. W., Bloomer, A. C., Petsko, G. A., Phillips, D. C., Pogson, C. I., Wilson, I. A., Coran, P. H., Furth, A. J., Milman, J. D., Offord, R. E., Priddle, J. D., and Waley, S. G. (1975) *Nature 255*, 609−614.
8. Knowles, J. R. (1991) *Nature 350*, 121−124.
9. Sun, A. Q., Yuksel, K. U., and Gracy, R. W. (1992) *Arch. Biochem. Biophys. 295*, 421−428.
10. Borchert, T. V., Abagyan, R., Jaenicke, R., and Wierenga, R. K. (1994) *Proc. Natl. Acad. Sci. U.S.A. 91*, 1515−1518.
11. Borchert, T. V., Abagyan, R., Radha Kishan, K. V., Zeelan, J. P., and Wierenga, R. K. (1993) *Structure 1*, 205−213.
12. Schliebs, W., Thanki, N., Jaenicke, R., and Wierenga, R. K. (1997) *Biochemistry 36*, 9655−9662.
13. Miles, E. W., Yutani, K., and Ogasahara, T. (1982) *Biochemistry 21*, 2586−2592.
14. Chryunk, B. A., and Matthews, C. R. (1990) *Biochemistry 29*, 2149−2154.
15. Godzik, A., Skolnick, J., and Kolinski, A. (1992) *Proc. Natl. Acad. Sci. U.S.A. 89*, 2629−2633.
16. Rudolph, R., Siebendritt, R., and Kiefhaber, T. (1992) *Protein Sci. 1*, 654−666.
17. Luger, K., Hommel, U., Herold, M., Hofsttenge, M., and Kirschner, K. (1989) *Science 243*, 206−210.
18. Knowles, J. R., and Albery, W. J. (1977) *Acc. Chem. Res.* 10, 105−111.
19. Blacklow, S. C., and Knowles, J. R. (1990) *Biochemistry 19*, 472−477.
20. Sun, A. Q., Yuksel, K. U., and Gracy, R. W. (1992) *Arch. Biochem. Biophys. 293*, 382−390.
21. Sepulveda-Becerra, M. A., Ferreira, S. T., Strasser, R. J., Garzon-Rodriguez, W., Beltran, C., Gomez-Puyou, A., and Darszon, A. (1996) *Biochemistry 35*, 15915−15922.
22. Sun, A. Q., Yuksel, K. U., and Gracy, R. W. (1992) *Arch. Biochem. Biophys. 295*, 421−428.
23. Zabori, S., Rudolph, R., and Jaenicke, R. (1980) *Z. Naturforsch. 35*, 999−1004.
24. Mainfroid, V., Terpson, P., Beauregard, M., Frere, J. M., Mande, S. C., Hol, W. G. J., Marshall, J. A., and Goraj, K. (1996) *J. Mol. Biol. 257*, 441−456.
25. Mainfroid, V., Mande, S. C., Hol, W. G., Martial, J. A., and Goraj, K. (1996) *Biochemistry 35*, 4110−4117.
26. Ranie, J., Kumar, V. P., and Balaram, H. (1993) *Mol. Biochem. Parasitol. 61*, 159−170.
27. Velankar, S. S., Ray, S. S., Gokhale, R. S., Suma, S., Balaram, H., Balaram, P., and Murthy, M. R. N. (1997) *Structure 5*, 751−761.
28. Hol, W. G. J., Vellieux, F. M. D., Verlinde, C. L. M. J., Wierenga, R. K., Nobel, M. E. M, and Read, R. J. (1991) in *Molecular Conformations and Biological Interactions* (Balaram, P., and Ramaseshan, S., Eds.) pp 215−240, Indian Academy of Sciences, Bangalore, India.
29. Anderson, A., and Cooper, R. A. (1970) *J. Gen. Microbiol. 62*, 329−334.
30. Kunkel, T. A. (1985) *Proc. Natl. Acad. Sci. U.S.A. 82*, 367−371.
31. Ellman, G. L. (1959) *Arch. Biochem. Biophys. 82*, 70−77.
32. Forman, M. D., Stack, R. F., Masters, C. R. H., and Baxter, S. M. (1998) *Protein Sci. 7*, 500−503.
33. Calderone, T. L., Stevens, R. D., and Oas, T. G. (1996) *J. Mol. Biol. 262*, 407−412.
34. Lakowicz, J. R. (1983) *Principles of Fluorescence Spectroscopy*, Plenum Press, New York.
35. Logan, T. M., Olejniczak, E. T., Xu, F. X., and Fesik, S. W. (1993) *J. Biomol. NMR* 3, 225−231.
36. Neri, D., Wider, G., and Wuthrich, K. (1992) *FEBS Lett. 303*, 129−135.
37. Jaenicke, R. (1987) *Prog. Biophys. Mol. Biol. 49*, 117−237.
38. Peters, C. D., Walsh, A. G., and Beauregard, M. (1997) *Biochem. Cell. Biol. 75*, 55−61.
39. Pohl, M., Grotzinger, J., Wollmer, A., and Kula, M. (1994) *Eur. J. Biochem. 224*, 651−661.
40. Liang, S. J., Lin, Y. Z., Zhou, J. M., Tsou, C. L., Wu, P. Q., and Zhou, Z. K. (1990) *Biochim. Biophys. Acta 1038*, 240−246.
41. West, S. M., Rice, J. E., Beaumont, E. S., Kelly, S. M., Price, N. C., and Lindsay, J. G. (1995) *Biochem. J. 308* (Pt 3), 1025−1029.
42. Schumann, J., and Jaenicke, R. (1993) *Eur. J. Biochem. 213*, 1225−1233.
43. Horowitz, P., and Criscimagna, N. L. (1986) *J. Biol. Chem. 261*, 15652−15658.
44. Sowdhamini, R., Srinivasan, N., Shoichet, B., Santi, D. V., Ramakrishnan, C., and Balaram, P. (1989) *Protein Eng. 3*, 95−103.
45. Galat, A., Creighton, T. E., Lord, R. C., and Blout, E. R. (1981) *Biochemistry 20*, 594−601.
46. Staley, J. P., and Kim, P. S. (1994) *Protein Sci. 3*, 1822−1832.
47. Ewbank, J. J., and Creighton, T. E. (1993) *Biochemistry 32*, 3677−3693.
48. Smith, J. S., and Scholtz, J. M. (1996) *Biochemistry 35*, 7292−7297.
49. Makhatadze, G. I., and Privalov, P. L. (1992) *J. Mol. Biol. 226*, 491−505.
50. Pace, C. N., Laurents, D. V., and Thomson, J. A. (1990) *Biochemistry 29*, 2564−2572.
51. Bowie, J. U., and Sauer, R. T. (1989) *Biochemistry 28*, 7139−7143.
52. Kellis, J. T., Jr., Nyberg, K., and Fersht, A. R. (1988) *Biochemistry 28*, 4914−4922.
53. Khurana, R., and Udgaonkar, J. B. (1994) *Biochemistry 33*, 106−115.
54. Santoro, M. M., and Bolen, D. W. (1988) *Biochemistry 27*, 8063−8068.
55. Liu, G., Topping, J. B., Cover, W. H., and Randall, L. L. (1988) *J. Biol. Chem. 263*, 14790−14793.
56. Chun, S. Y., Strobel, S., Bassford, Jr., and Randall, L. L. (1993) *J. Biol. Chem. 268*, 20855−20862.
57. Fredricksen, R. S., and Swenson, C. A. (1996) *Biochemistry 35*, 14012−14026.
58. Yu, X. C., Shen, S., and Strobel, H. W. (1995) *Biochemistry 34*, 5511−5517.
59. Klug, C. S., Su, W., Liu, J., Klebba, P. E., and Feix, J. B. (1995) *Biochemistry 34*, 14230−14236.
60. Nishii, I., Kataoka, M., and Goto, Y. (1995) *J. Mol. Biol. 250*, 223−238.
61. Matthews, C. R., and Crisanti, M. M. (1981) *Biochemistry 20*, 784−792.
62. Kelly, R., Wilson, J., Bryant, C., Shaongo, W., Ledger, R., Lowery, D., and Stellwagon, E. (1986) *Thioredoxin & Glutaredoxin System: Structure and Function* (Holmgren, A., Ed.) Raven Press, New York.
63. Holzman, T. S., Brems, D. N., and Dougherty, J. G., Jr. (1986) *Biochemistry 25*, 6907−6917.
64. Brems, D. N., Plaisted, S. M., Havel, H. A., and Tomich, C. C. (1988) *Proc. Natl. Acad. Sci. U.S.A. 85*, 3367−3371.
65. Kern, G., Schulke, N., Schmid, F. X., and Jaenicke, R. (1992) *Protein Sci. 1*, 120−131.
66. Aceto, A., Caccuri, A. M., Sacchelta, P., Bucciarelli, J., Dragani, B., Rosato, N., Fedirici, G., and Doilo, C. (1992) *Biochem. J. 285*, 241−245.
67. Lambeir, A. M., Diaz Pereira, J. F., Chacon, P., Vermeulen, G., Heremans, K., Devreese, B., Van Beeumen, J., De Meester, I., and Scharpe, S. (1997) *Biochim. Biophys. Acta 1340*, 215−226.
68. Zhuang, P., Li, H., Williams, J. G., Wagner, N. V., Seiffert, D., and Peterson, C. B. (1996) *J. Biol. Chem. 271*, 14333−14343.
69. Bras, G. L., Teschner, W., Deville-Bonne, D., and Garel, J. R. (1989) *Biochemistry 28*, 6836−6841.

BI981087S